The Astrophysical Journal Letters, 973:L34 (6pp), 2024 September 20 https://doi.org/10.3847/2041-8213/ad772e

Observation of the Galactic Center PeVatron beyond 100 TeV with HAWC

A. Albert[1], R. Alfaro[2], C. Alvarez[3], A. Andrés[4], J. C. Arteaga-Velázquez[5], D. Avila Rojas[2], H. A. Ayala Solares[6], R. Babu[7], E. Belmont-Moreno[2], A. Bernal[4], K. S. Caballero-Mora[3], T. Capistrán[4], A. Carramiñana[8], S. Casanova[9], U. Cotti[5], J. Cotzomi[10], S. Coutiño de León[11], E. De la Fuente[12], C. de León[5], D. Depaoli[13], N. Di Lalla[14], R. Diaz Hernandez[8], B. L. Dingus[1], M. A. DuVernois[11], J. C. Díaz-Vélez[11], K. Engel[15], T. Ergin[7], C. Espinoza[2], K. L. Fan[15], K. Fang[11], N. Fraija[4], S. Fraija[4], J. A. García-González[16], F. Garfias[4], H. Goksu[13], M. M. González[4], J. A. Goodman[15], S. Groetsch[17], J. P. Harding[1], S. Hernández-Cadena[18], I. Herzog[7], J. Hinton[13], D. Huang[15], F. Hueyotl-Zahuantitla[3], T. B. Humensky[19], P. Hüntemeyer[17], A. Iriarte[4], S. Kaufmann[20], D. Kieda[21], A. Lara[22], W. H. Lee[4], J. Lee[23], H. León Vargas[2], J. T. Linnemann[7], A. L. Longinotti[4], G. Luis-Raya[20], K. Malone[1], O. Martinez[10], J. Martínez-Castro[24], J. A. Matthews[25], P. Miranda-Romagnoli[26], J. A. Montes[4], J. A. Morales-Soto[5], E. Moreno[10], M. Mostafá[27], M. Najafi[17], L. Nellen[28], M. Newbold[21], M. U. Nisa[7], R. Noriega-Papaqui[26], L. Olivera-Nieto[13], N. Omodei[14], M. Osorio-Archila[2], Y. Pérez Araujo[2], E. G. Pérez-Pérez[20], C. D. Rho[29], D. Rosa-González[8], E. Ruiz-Velasco[13], H. Salazar[10], D. Salazar-Gallegos[7], A. Sandoval[2], M. Schneider[15], G. Schwefer[13], J. Serna-Franco[2], A. J. Smith[15], Y. Son[23], R. W. Springer[21], O. Tibolla[20], K. Tollefson[7], I. Torres[8], R. Torres-Escobedo[18], R. Turner[17], F. Ureña-Mena[8], E. Varela[10], X. Wang[17], Z. Wang[15], I. J. Watson[23], E. Willox[15], H. Wu[11], S. Yu[6], S. Yun-Cárcamo[15], and H. Zhou[18]

[1] Los Alamos National Laboratory, Los Alamos, NM, USA
[2] Instituto de Física, Universidad Nacional Autónoma de México, Ciudad de México, Mexico
[3] Universidad Autónoma de Chiapas, Tuxtla Gutiérrez, Chiapas, Mexico
[4] Instituto de Astronomía, Universidad Nacional Autónoma de México, Ciudad de México, Mexico
[5] Universidad Michoacana de San Nicolás de Hidalgo, Morelia, Mexico
[6] Department of Physics, Pennsylvania State University, University Park, PA, USA
[7] Department of Physics and Astronomy, Michigan State University, East Lansing, MI, USA; baburish@msu.edu
[8] Instituto Nacional de Astrofísica, Óptica y Electrónica, Puebla, Mexico
[9] Instytut Fizyki Jadrowej im Henryka Niewodniczanskiego Polskiej Akademii Nauk, IFJ-PAN, Krakow, Poland
[10] Facultad de Ciencias Físico Matemáticas, Benemérita Universidad Autónoma de Puebla, Puebla, Mexico
[11] Department of Physics, University of Wisconsin-Madison, Madison, WI, USA
[12] Departamento de Física, Centro Universitario de Ciencias Exactase Ingenierias, Universidad de Guadalajara, Guadalajara, Mexico
[13] Max-Planck Institute for Nuclear Physics, 69117 Heidelberg, Germany
[14] Department of Physics, Stanford University: Stanford, CA 94305-4060, USA
[15] Department of Physics, University of Maryland, College Park, MD, USA; klfan@terpmail.umd.edu, dezhih@umd.edu, yunsoh@umd.edu
[16] Tecnologico de Monterrey, Escuela de Ingenieria y Ciencias, Ave. Eugenio Garza Sada 2501, Monterrey, N. L., 64849, Mexico
[17] Department of Physics, Michigan Technological University, Houghton, MI, USA
[18] Tsung-Dao Lee Institute & School of Physics and Astronomy, Shanghai Jiao Tong University, People's Republic of China
[19] NASA Goddard Space Flight Center, Greenbelt, MD 20771, USA
[20] Universidad Politecnica de Pachuca, Pachuca, Hgo, Mexico
[21] Department of Physics and Astronomy, University of Utah, Salt Lake City, UT, USA
[22] Instituto de Geofísica, Universidad Nacional Autónoma de México, Ciudad de México, Mexico
[23] University of Seoul, Seoul, Republic of Korea
[24] Centro de Investigación en Computación, Instituto Politécnico Nacional, México City, Mexico
[25] Dept of Physics and Astronomy, University of New México, Albuquerque, NM, USA
[26] Universidad Autónoma del Estado de Hidalgo, Pachuca, Mexico
[27] Department of Physics, Temple University, Philadelphia, PA, USA
[28] Instituto de Ciencias Nucleares, Universidad Nacional Autónoma de México, Ciudad de México, Mexico
[29] Department of Physics, Sungkyunkwan University, Suwon 16419, Republic of Korea

Received 2024 July 4; revised 2024 August 29; accepted 2024 September 3; published 2024 September 20

Abstract

We report an observation of ultrahigh-energy (UHE) gamma rays from the Galactic center (GC) region, using 7 yr of data collected by the High-Altitude Water Cherenkov (HAWC) Observatory. The HAWC data are best described as a point-like source (HAWC J1746-2856) with a power-law spectrum ($dN/dE = \phi(E/26\,\mathrm{TeV})^{\gamma}$), where $\gamma = -2.88 \pm 0.15_{\mathrm{stat}} - 0.1_{\mathrm{sys}}$ and $\phi = 1.5 \times 10^{-15}$ $(\mathrm{TeV\,cm^2\,s})^{-1}$ $\pm 0.3_{\mathrm{stat}}\,^{+0.08_{\mathrm{sys}}}_{-0.13_{\mathrm{sys}}}$ extending from 6 to 114 TeV. We find no evidence of a spectral cutoff up to 100 TeV using HAWC data. Two known point-like gamma-ray sources are spatially coincident with the HAWC gamma-ray excess: Sgr A* (HESS J1745-290) and the Arc (HESS J1746-285). We subtract the known flux contribution of these point sources from the measured flux of HAWC J1746-2856 to exclude their contamination and show that the excess observed by HAWC remains significant ($>5\sigma$), with the spectrum extending to >100 TeV. Our result supports that these detected UHE gamma rays can originate via hadronic interaction of PeV cosmic-ray protons with the dense ambient gas and confirms the presence of a proton PeVatron at the GC.

Unified Astronomy Thesaurus concepts: Galactic center (565); Gamma-rays (637); Ultra-high-energy cosmic radiation (1733)

1. Introduction

The Galactic sources of cosmic-ray acceleration to petaelectronvolt (PeV) energies—known as PeVatrons—remain unidentified and are still subject to discussion (P. Blasi 2013; E. Amato 2014; F. Aharonian et al. 2019; S. Gabici et al. 2019; P. Cristofari 2021; T. Sudoh & J. F. Beacom 2023; E. de Oña Wilhelmi et al. 2024; K. Fang & F. Halzen 2024). Previous studies suggest that cosmic rays are actively accelerated in the Galactic center (GC) region (H.E.S.S. Collaboration et al. 2016). The arc-minute angular resolution of the Imaging Atmospheric Cherenkov Telescopes (IACTs), e.g., the High Energy Stereoscopic System (H.E.S.S.; F. Aharonian et al. 2006a; H.E.S.S. Collaboration et al. 2016; H. Abdalla et al. 2018), the Major Atmospheric Gamma-Ray Imaging Cherenkov (MAGIC) telescopes (V. A. Acciari et al. 2020), and the Very Energetic Radiation Imaging Telescope Array System (VERITAS; C. B. Adams et al. 2021), has allowed them to measure gamma-ray emission up to ∼20 TeV from the two point sources of interest in the region: Sgr A* (HESS J1745-290), the supermassive black hole at the center of the Galaxy, and the unidentified source HESS J1746-285, which is spatially coincident with the Galactic radio arc (F. Yusef-Zadeh & M. Morris 1987; F. Yusef-Zadeh et al. 2004). The observation of the point-like supernova remnant (SNR) G0.9+0.1 (H. Abdalla et al. 2018; V. A. Acciari et al. 2020; C. B. Adams et al. 2021) and the unidentified extended-source HESS J1745-303 (F. Aharonian et al. 2006b) was reported as well about 1° away from the GC. These IACTs have also observed very high-energy (VHE) gamma rays from the GC ridge (H.E.S.S. Collaboration et al. 2016; H. Abdalla et al. 2018; V. A. Acciari et al. 2020; C. B. Adams et al. 2021). This diffuse emission spatially correlates to the Central Molecular Zone (CMZ) morphology (F. Aharonian et al. 2006b), which is derived from dense gas tracers (M. Tsuboi et al. 1999). This correlation suggests a hadronic origin for the observed gamma-ray emission given the severe energy losses via synchrotron emission in the leptonic scenario (F. Aharonian et al. 2006a; H.E.S.S. Collaboration et al. 2016; H. Abdalla et al. 2018).

In this work, we use 7 yr of data from the High-Altitude Water Cherenkov (HAWC) Gamma-Ray Observatory to study the gamma-ray emission from the GC region. Our analysis extends the previous observations to energies >100 TeV, which allows the PeV cosmic-ray interaction to be directly probed. We show that the ultrahigh-energy (UHE) emission observed by HAWC is most likely from the Galactic ridge emission by subtracting the flux contribution from HESS J1745-290, as reported in H.E.S.S. Collaboration et al. (2016), with good agreement in location and spectrum to other observations (V. A. Acciari et al. 2020; C. B. Adams et al. 2021; K. Abe et al. 2023), and from HESS J1746-285, as reported in H. Abdalla et al. (2018). The latter has been observed by several IACTs also with good agreement, but only in H. Abdalla et al. (2018) is the contribution of underlying diffuse emission additionally taken into account for the source HESS J1746-285. The flux contribution of these two sources at energies >100 TeV is extremely small. This indicates that these sources do not contribute solely to the origin of the observed VHE gamma rays. Our result provides evidence of a PeVatron at the center of our Galaxy with the first measurement of nearly 100 gamma-ray events with energies >100 TeV.

This Letter is organized as follows: Section 2 briefly describes the HAWC data set used in this analysis, Sections 3 and 4 present and discuss the results of the analysis, and in Section 5 we present our conclusions.

2. HAWC Data

The HAWC Observatory—located on the side of the Sierra Negra volcano in Puebla, Mexico, at 4100 m above sea level—is made up of 300 water Cherenkov detectors (A. U. Abeysekara et al. 2023). We apply signal topology-based cuts to reduce the cosmic-ray background (99.9% of events detected). We recently updated HAWC's reconstruction algorithms ("Pass 5"), improving its effective area, angular resolution, and gamma/hadron separation at the highest energies and zenith angles. With these improvements, HAWC is able to observe the GC, which culminates at 48° zenith (A. Albert et al. 2024). As a further check, we verified that the results obtained when reconstructing data from the Crab Nebula when it reaches zenith angles greater than 45° are in agreement with those reported in the study by A. Albert et al. (2024).

Using 2546 days of HAWC data, we detected gamma-ray emission from the GC region, with a maximum significance of 6.5σ above the background. We analyzed the data with the Pass 5 version of the neural network energy estimator (A. U. Abeysekara et al. 2019; A. Albert et al. 2024) and included off-array events, which are showers whose cores fall off the main array up to 1.5 times its physical area and improve the sensitivity of HAWC to high zenith angles and high energies (A. Albert et al. 2024).

To model the gamma-ray flux from the GC region, we employed the HAWC Accelerated Likelihood plug-in with the Multi-Mission Maximum Likelihood (3ML)[30] framework (P. W. Younk et al. 2015; A. U. Abeysekara et al. 2022)—a forward-folded maximum-likelihood approach (G. Vianello et al. 2016)—within a rectangular region of interest ±3° in latitude and ±2.°5 in longitude.

We define our test statistic (TS) as

$$\mathrm{TS} = 2\ln\left(\frac{L_{\mathrm{model}}}{L_{\mathrm{bkg}}}\right), \tag{1}$$

where L_{model} denotes the maximum likelihood from the source model and L_{bkg} is background only. According to Wilks' theorem (S. S. Wilks 1938), which applies to HAWC data (A. U. Abeysekara et al. 2017), the TS is asymptotically χ^2 distributed, with the degrees of freedom equal to the difference in the number of free parameters of the nested models. Thus, under the case of one free parameter, $\sqrt{\mathrm{TS}}$ can be used as a measure of significance, σ.

The extended-source assumption was tested, and no strong preference was found ($\Delta\mathrm{TS} = 6.62$ compared to the point-source assumption); hence, the simplest model was chosen. From the extended-source fit, we estimated an upper limit (UL) on the source extension (radius) at the 68% confidence level

[30] https://github.com/threeML/threeML

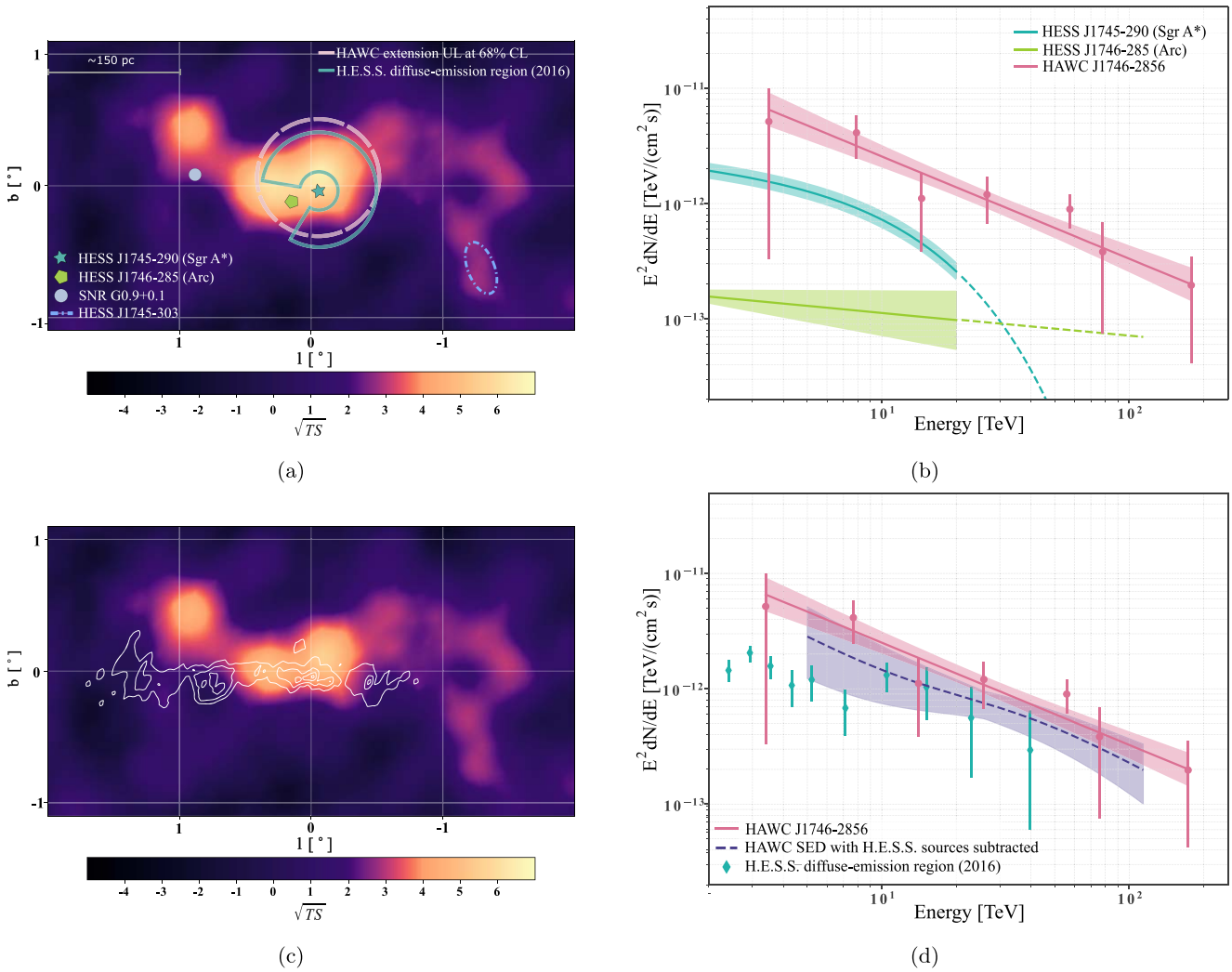

Figure 1. GC analysis results. (a) Significance map obtained using the HAWC neural network energy estimator (on- and off-array events; A. U. Abeysekara et al. 2019) and the position of the three main point sources and one extended source in the GC region as measured by H.E.S.S.. The dashed circle outlines the extension UL at the 68% CL. We also include the diffuse region used in the H.E.S.S. analysis (H.E.S.S. Collaboration et al. 2016). (b) Spectra of the two H.E.S.S. sources, along with the best-fit spectrum of HAWC J1746-2856. The dashed lines for the H.E.S.S. sources show the extrapolation of their best fit to the HAWC energy range. The flux points are calculated for each energy bin (A. Albert et al. 2024) by fixing all the fit parameters except for the flux normalization. (c) HAWC emission after subtracting the two H.E.S.S. point sources. We also show the density distribution contours of the ambient gas as traced by CS (J1-0) line emission (M. Tsuboi et al. 1999). (d) Original best-fit HAWC spectral energy distribution and the result after subtracting the two H.E.S.S. point-source spectra. As a reference, we include the diffuse emission measured by H.E.S.S. Collaboration et al. (2016), as their region is almost spatially coincident with our model. See Section 3 for details.

(CL) for the Gaussian width of the source ($\sim 0.^{\circ}46$; see the dashed circle in Figure 1(a)). Adding curvature to the spectrum did not significantly improve the TS either ($\Delta \mathrm{TS} = 0.44$).

3. Main Analysis Results

The best fit to the data is a point source with a simple power-law spectrum (TS =49 for four free parameters—position and spectral parameters):

$$\frac{dN}{dE} = \phi\left(\frac{E}{26\ \mathrm{TeV}}\right)^{\gamma}, \tag{2}$$

where ϕ is the flux normalization at the pivot energy and γ is the power-law index. The pivot energy of 26 TeV is calculated such that it minimizes the correlation between the flux normalization and spectral index. We summarize the best-fit parameters of HAWC J1746-2856 in Table 1 and include both statistical and systematic uncertainties. The latter account for the contribution of four nonnegligible independent systematic uncertainties that were identified in the previous energy-dependent study of the Crab (A. U. Abeysekara et al. 2019) and

Table 1
Best-fit Results for HAWC J1746-2856 with Statistical and Systematic Uncertainties

Parameter Estimated	Best Fit	Statistical Uncertainties	Systematic Uncertainties
R.A. (°)	266.28	±0.05	+0.09, −0.06
Decl. (°)	−28.94	±0.04	+0.03, −0.02
Flux norm. (ϕ) $\times 10^{-15}$ (TeV cm^2 s)$^{-1}$	1.5	±0.30	+0.08, −0.13
Index (γ)	−2.88	±0.15	−0.1

Note. The spectrum is best described by a simple power law $dN/dE = \phi(E/26\ \mathrm{TeV})^{\gamma}$. See Section 3 for details. In Galactic coordinates, the best-fit position of HAWC J1746-2856 is $(l, b) = (0.^{\circ}06, 0.^{\circ}09)$.

are estimated by producing instrument response functions (IRFs) with different detector configurations to investigate any potential mismodeling of the detector. The results were then compared with the standard HAWC analysis, and the uncertainties were added in quadrature. Another source of systematic uncertainty in the flux of HAWC J1746-2856 could be emission from background cosmic rays, often referred to as the cosmic-ray sea, which is thought to have a consistent energy density throughout the Galaxy. Locally, above 100 TeV, the energy density of the cosmic-ray spectrum is approximately 3×10^{-4} eV cm^{-3} (M. Aguilar et al. 2015). For the diffuse emission to significantly impact the results, one would need to assume that the cosmic-ray sea's flux is nearly a factor of 10 higher at the GC. Even assuming an unusual spectral dependence or normalization of the diffusion coefficient within the CMZ, it would be difficult to explain the at least tenfold discrepancy between the reported local spectrum and the CMZ spectrum observed by HAWC. Additionally, the spectral indices of the cosmic-ray sea and HAWC J1746-2856 are not compatible. Thus, we keep the simplest point-source model.

We calculated a UL on the minimum energy at 6 TeV and a lower limit on the maximum energy at 114 TeV, both at the 68% CL. Above 100 TeV, the significance of the signal is 1.2σ. Above 100 TeV, 3474 events passed trigger conditions for reconstruction, from which 98 events passed HAWC gamma/hadron separation cuts. At 100 TeV, the energy resolution is 10% in $\log_{10}(E/\mathrm{TeV})$ (A. U. Abeysekara et al. 2019), and the hadron retention after gamma/hadron separation cuts is <1%. To count the events, we used a circular region centered in the best-fit position (see Table 1) with the radius set at the UL on the source extension.

In Figure 1(a), we show a significance map from the GC region obtained with HAWC data by calculating the TS of every pixel as the ratio of the logarithm of the likelihoods of the signal measured over the expected background (P. W. Younk et al. 2015; A. Abeysekara et al. 2017). We also include the location of HESS J1745-290 (Sgr A*; F. Aharonian et al. 2006b) and HESS J1746-285 (the Arc; H. Abdalla et al. 2018), which are relevant to this study as they are inside of the HAWC J1746-2856 extension UL radius and excluded from the diffuse emission region used in H.E.S.S. Collaboration et al. (2016). In addition, we show the positions of SNR G0.9+0.1 and HESS J1745-303. The reported gamma-ray flux level of the SNR falls below the sensitivity of HAWC at this decl. (A. Albert et al. 2024). No significant excess is observed by HAWC at the reported location of the SNR or HESS J1745-303. The 4.5σ hot spot above the SNR location is not coincident with any known gamma-ray sources, but it aligns with a candidate open stellar cluster (C. M. Dutra et al. 2003). Although gamma rays are observed in the vicinity of stellar clusters (A. Abramowski et al. 2012; A. U. Abeysekara et al. 2021; F. Aharonian et al. 2022), the analysis cannot rule out contributions from other unresolved sources.

Figure 1(b) shows the best-fit spectrum for HAWC J1746-2856 (see Table 1 for systematic uncertainties and best-fit position) compared to the H.E.S.S.-measured spectra of Sgr A* and the radio Arc. Since HAWC cannot resolve these point sources, we conservatively assume that their spectra extend and cover the entire HAWC energy range, which is represented with dashed lines in Figure 1(b). In Figure 1(c), we show the significance map obtained after subtracting the estimated excess of the H.E.S.S. point sources from the HAWC data. The predicted event count is calculated by convolving a model consisting of the reported best-fit parameters for the H.E.S.S. sources with the HAWC IRF. We also include contours of carbon monosulfide (CS) line emission—integrated from −200 to 200 km s^{-1}—to show the spatial correlation of the HAWC central excess with the density distribution of the ambient dense gas (M. Tsuboi et al. 1999). Thus, the residual shown in Figure 1(c) is likely emission from the GC ridge diffusion and, in smaller contribution, unresolved sources.

In Figure 1(d), we subtract the flux from the two H.E.S.S. point sources from the HAWC best-fit spectrum (shown separately in Figure 1(b)). The error band illustrates the combination of HAWC and H.E.S.S. uncertainties in quadrature. We also compare our measurement with the diffuse emission flux points estimated in H.E.S.S. Collaboration et al. (2016), where the diffuse emission was derived within an annulus of inner radius 0.°15—to exclude HESS J1745-290—and outer radius 0.°45. In that study, a sector (∼66°) of the annulus is excluded to avoid HESS J1746-285. These excluded regions and the slightly larger radius of the HAWC source (0.°46) may explain the higher flux detected by HAWC, although both results are still compatible within uncertainties (see Figure 1(d)). The hard spectrum reported by H.E.S.S. with a photon index of 2.3 (H.E.S.S. Collaboration et al. 2016) is mostly dominated by events with energies below 10 TeV. HAWC is more sensitive at higher energies and measures an index of 2.9. The change in the spectral index occurs at low energies where HAWC is not sensitive enough to probe the cause, given the large zenith angle. However, we find no evidence of significant spectral curvature from 10s of TeV to 114 TeV. Other IACTs have also measured the diffuse emission. However, they use regions with significantly different morphologies: in the studies by H.E.S.S. (H. Abdalla et al. 2018) and MAGIC (V. A. Acciari et al. 2020) the entire $l \leqslant |\pm 1^\circ|$ GC region is included, while in VERITAS, C. B. Adams et al. (2021) utilized seven circular regions of 0.°1 radius outside of the H.E.S.S. (H.E.S.S. Collaboration et al. 2016) annuli.

In summary, we have shown that the measured flux of HAWC J1746-2856 is significantly higher than that of HESS J1745-290 and HESS J1746-285. Therefore, even after excluding their contributions, the spectrum extends beyond 100 TeV.

4. Discussion

The HAWC detection of photons with energies exceeding 100 TeV further strengthens the hadronic-origin interpretation suggested by H.E.S.S. Collaboration et al. (2016), where relativistic protons ($\gtrsim$1 PeV) collide with the surrounding dense ambient gas.

In the leptonic scenario, the gamma-ray emission comes from the inverse Compton scattering of electrons with energies $E_e > 100$ TeV. In the GC region, these electrons have a short lifetime, mostly due to synchrotron radiation. Assuming a magnetic field strength of 100 μG (R. M. Crocker et al. 2010), the cooling time is

$$t_{\mathrm{cool}} \approx 13 \left(\frac{E_{\mathrm{e}}}{100\ \mathrm{TeV}} \right)^{-1} \left(\frac{B}{100\ \mu\mathrm{G}} \right)^{-2} \mathrm{yr}, \quad (3)$$

corresponding to a maximum distance that the electrons may travel $c\, t_{\mathrm{cool}} = 4$ pc, even assuming the extreme case of ballistic movement. Such a distance is significantly smaller than the size

of the CMZ, which is hundreds of parsec. Therefore, the HAWC observation strongly disfavors the leptonic scenario. The only way to make such a scenario work would be to have tens of unresolved electron accelerators coexisting in the region.

In the hadronic scenario, although π_0 decay is the dominant cool-down channel (F. Aharonian et al. 2009; M. S. Longair 2010), the cooling time is so much larger than the escape time (by several orders of magnitude) that the proton-cooling effect is negligible (A. Scherer et al. 2023). The escape time of $E_{\rm p} = 1$ PeV protons can be roughly estimated as

$$t_{\rm escape} \approx \frac{r^2}{2D} \approx 100 \left(\frac{r}{40\ {\rm pc}}\right)^2 \left(\frac{E_{\rm p}}{1\ {\rm PeV}}\right)^{-0.3} {\rm yr}, \quad (4)$$

where $D \sim 1.2 \times 10^{30} (E_{\rm p}/100\ {\rm TeV})^{0.3}\ {\rm cm^2\ s^{-1}}$ (A. W. Strong et al. 2007) is the diffusion coefficient in the interstellar medium (ISM) and $r \sim 40$ pc is the radius of the diffuse emission region used in H.E.S.S. Collaboration et al. (2016). As the magnetic field at the GC is much higher than that of the average ISM (R. M. Crocker et al. 2010), protons are likely confined therein for a longer time. Nonetheless, $t_{\rm escape}$ is much shorter than the age of the Galaxy, implying that the proton source(s) are either very young or injecting protons into the CMZ in a recent burst. Therefore, the only plausible explanation is that one or more sources quasi-continuously accelerate and inject high-energy protons into the CMZ at rates that exceed the escape time.

Finally, we estimated the gamma-ray luminosity ($L_\gamma(E_\gamma \geqslant 10\ {\rm TeV}) = 2.24 \times 10^{34}\ {\rm erg\ s^{-1}}$) by integrating the differential flux of the HAWC central source between 10 and 114 TeV, subtracting the contribution of H.E.S.S. point sources and assuming an 8.5 kpc distance to the GC region. With this result, we calculated the energy density of cosmic-ray protons using our measurement of the gamma-ray flux above 10 TeV to be

$$\begin{aligned} w_{\rm p}(\geqslant 10 E_\gamma) &= 1.8 \times 10^{-2} \left(\frac{\eta_N}{1.5}\right)^{-1} \left(\frac{L_\gamma(E_\gamma \geqslant 10\ {\rm TeV})}{10^{34}\ {\rm erg\ s^{-1}}}\right) \\ &\quad \times \left(\frac{M}{10^6 M_\odot}\right)^{-1} {\rm eV\ cm^{-3}} \\ &\approx 8.1 \times 10^{-3}\ {\rm eV\ cm^{-3}}, \end{aligned} \quad (5)$$

where the CS total mass of the gas ($5 \times 10^6 M_\odot$) is the sum of CS mass in the three H.E.S.S. annuli that are roughly coincident with the HAWC region (H.E.S.S. Collaboration et al. 2016) and $\eta_N = 1.5$ considers the existence of nuclei heavier than hydrogen in cosmic rays and the interstellar matter. This energy density obtained for >100 TeV protons is larger than the $1 \times 10^{-3}\ {\rm eV\ cm^{-3}}$ local measurement by the Alpha Magnetic Spectrometer (M. Aguilar et al. 2015; A. U. Abeysekara et al. 2021). Additionally, we calculate the total energy budget of protons with energies >100 TeV:

$$W_p \approx L_\gamma(E_\gamma \geqslant 10\ {\rm TeV})\, t_{\rm pp} \approx 3.53 \times 10^{49} n^{-1}\ {\rm erg}, \quad (6)$$

where $t_{\rm pp} \approx 5 \times 10^7 n^{-1}$ yr is the cooling time for proton–proton (pp) interactions assuming the relative velocity of the interacting protons to be equivalent to the speed of light (c) and an ambient gas density of n, in units of ${\rm cm^{-3}}$. We estimated the cosmic-ray energy density from H.E.S.S. measurements using the diffuse region shown in Figure 1. By integrating the protons with energies between 100 and 1140 TeV, we found the integral cosmic-ray density to be $\approx 2.1 \times 10^{49} n^{-1}$ erg, which is compatible with HAWC's results. Our interpretation is consistent with the steady proton source scenario suggested by H.E.S.S. Collaboration et al. (2016). Therefore, we attribute the UHE gamma rays to the freshly accelerated proton cosmic rays from the local accelerators within the GC region, which continuously inject protons with PeV energies.

5. Conclusions

We report the first detection of >100 TeV gamma rays from the GC region with a number of nearly 100 events. This HAWC result extends the highest energy reported from the GC by the IACTs by more than a factor of 2. The best-fit model for 7 yr of HAWC data from the GC is a point source with a simple power-law spectrum ($dN/dE = \phi(E/26\ {\rm TeV})^\gamma$), where $\gamma = -2.88 \pm 0.15_{\rm stat} - 0.1_{\rm sys}$ and $\phi = 1.5 \times 10^{-15}$ $({\rm TeV\ cm^2\ s})^{-1} \pm 0.3_{\rm stat}\ ^{+0.08}_{-0.13}{}_{\rm sys}$, with no signs of a cutoff. After subtracting the small contribution of HESS J1745-290 and HESS J1746-285 from the HAWC best-fit spectrum, the remaining flux—likely from the Galactic ridge diffuse emission—maintains the power-law shape, extending to at least 114 TeV. Extending the power-law spectrum to these energies reveals a PeVatron at the GC, as first suggested by H.E.S.S. Collaboration et al. (2016), with photons up to ∼30 TeV. Although our analysis does not resolve the object accelerating protons to PeV energies, we can confirm the existence of a PeVatron at the GC. Additionally, we discuss the possible origin of such high-energy gamma rays—using model-independent arguments—and conclude that the hadronic mechanism and quasi-continuous injection scenarios are preferred. Moreover, we calculate the gamma-ray luminosity of the PeVatron and find that the cosmic-ray energy density is above the average, which clearly suggests the presence of freshly accelerated 0.1–1 PeV protons in the GC region. Finally, we show that the total energy budget of protons with energies >100 TeV calculated with HAWC data is compatible with H.E.S.S. measurements.

Several specific sites of proton acceleration have been proposed within the HAWC J1746-2856 emission region, in particular near the vicinity of Sgr A* (H.E.S.S. Collaboration et al. 2016) and within the compact star clusters, the Arches and Quintuplet clusters (F. Aharonian et al. 2019), which we did not resolve in this analysis. Recently, there has been progress in modeling the CMZ with more realistic cosmic-ray dynamics in agreement with existing data (A. Scherer et al. 2023). The next generation of experiments, such as the Cherenkov Telescope Array (The CTA Consortium et al. 2019) and the Southern Wide-field Gamma-ray Observatory (A. Albert et al. 2019), could better differentiate and constrain these models with improved gamma-ray observations.

Acknowledgments

We acknowledge the support from the US National Science Foundation (NSF); the US Department of Energy Office of High-Energy Physics; the Laboratory Directed Research and Development (LDRD) program of Los Alamos National Laboratory; Consejo Nacional de Ciencia y Tecnología (CONACyT), México,

grants 271051, 232656, 260378, 179588, 254964, 258865, 243290, 132197, A1-S-46288, A1-S-22784, CF-2023-I-645, cátedras 873, 1563, 341, 323; Red HAWC, México; DGAPA-UNAM, grants IG101323, IN111716-3, IN111419, IA102019, IN106521, IN114924, IN110521 , IN102223; VIEP-BUAP; PIFI 2012, 2013, PROFOCIE 2014, 2015; the University of Wisconsin Alumni Research Foundation; the Institute of Geophysics, Planetary Physics, and Signatures at Los Alamos National Laboratory; Polish Science Centre, grant DEC-2017/27/B/ST9/02272; Coordinación de la Investigación Científica de la Universidad Michoacana; Royal Society—Newton Advanced Fellowship 180385; Generalitat Valenciana, grant CIDEGENT/2018/034; The Program Management Unit for Human Resources & Institutional Development, Research and Innovation, NXPO (grant No. B16F630069); Coordinación General Académica e Innovación (CGAI-UdeG), PRODEP-SEP UDG-CA-499; National Research Foundation of Korea RS-2023-00280210; Consejo Nacional de Ciencia y Tecnología (CONACyT), México, grants LNC-2023-117; Institute of Cosmic Ray Research (ICRR), University of Tokyo. H.F. acknowledges support by NASA under award number 80GSFC21M0002. We also acknowledge the significant contributions over many years of Stefan Westerhoff, Gaurang Yodh, and Arnulfo Zepeda Domínguez, all deceased members of the HAWC collaboration. Thanks go to Scott Delay, Luciano Díaz, and Eduardo Murrieta for their technical support.

S.Y.-C. analyzed the data, performed the maximum likelihood analysis, and prepared the original Letter. S.Y.-C. and D.H. carried out the discussion section calculations. R.B., K.L.F., and D.H. helped with the analysis tools and interpretation of results. The full HAWC Collaboration has contributed through the construction, calibration, and operation of the detector, the development and maintenance of the reconstruction and analysis software, and vetting of the analysis presented in this Letter. All authors have reviewed, discussed, and commented on the results and the Letter.

ORCID iDs

R. Babu https://orcid.org/0000-0002-5529-6780
K. L. Fan https://orcid.org/0000-0002-8246-4751
D. Huang https://orcid.org/0000-0002-5447-1786
S. Yun-Cárcamo https://orcid.org/0000-0002-9307-0133

References

Abdalla, H., Abramowski, A., Aharonian, F., et al. 2018, A&A, 612, A9
Abe, K., Abe, S., Aguasca-Cabot, A., et al. 2023, in 38th Int. Cosmic Ray Conf. (ICRC2023) (Trieste: SISSA), 574
Abeysekara, A., Albert, A., Alfaro, R., et al. 2017, ApJ, 843, 39
Abeysekara, A. U., Albert, A., Alfaro, R., et al. 2017, ApJ, 843, 40
Abeysekara, A. U., Albert, A., Alfaro, R., et al. 2019, ApJ, 881, 134
Abeysekara, A. U., Albert, A., Alfaro, R., et al. 2021, NatAs, 5, 465
Abeysekara, A. U., Albert, A., Alfaro, R., et al. 2022, in Proc. 37th ICRC (Berlin: ICRC)
Abeysekara, A. U., Albert, A., Alfaro, R., et al. 2023, NIMPA, 1052, 168253
Abramowski, A., Acero, F., Aharonian, F., et al. 2012, A&A, 537, A114
Acciari, V. A., Ansoldi, S., Antonelli, L., et al. 2020, A&A, 642, A190
Adams, C. B., Benbow, W., Brill, A., et al. 2021, ApJ, 913, 115
Aguilar, M., Aisa, D., Alpat, B., et al. 2015, PhRvL, 114, 171103
Aharonian, F., Akhperjanian, A., Anton, G., et al. 2009, A&A, 503, 817
Aharonian, F., Akhperjanian, A., Bazer-Bachi, A., et al. 2006a, ApJ, 636, 777
Aharonian, F., Akhperjanian, A. G., Bazer-Bachi, A. R., et al. 2006b, Natur, 439, 695
Aharonian, F., Ashkar, H., Backes, M., et al. 2022, A&A, 666, A124
Aharonian, F., Yang, R., & de Oña Wilhelmi, E. 2019, NatAs, 3, 561
Albert, A., Alfaro, R., Alvarez, C., et al. 2024, ApJ, 972, 144
Albert, A., Alfaro, R., Ashkar, H., et al. 2019, arXiv:1902.08429
Amato, E. 2014, IJMPD, 23, 1430013
Blasi, P. 2013, A&ARv, 21, 70
Cristofari, P. 2021, Univ, 7, 324
Crocker, R. M., Jones, D. I., Melia, F., Ott, J., & Protheroe, R. J. 2010, Natur, 463, 65
de Oña Wilhelmi, E., López-Coto, R., Aharonian, F., et al. 2024, NatAs, 8, 425
Dutra, C. M., Ortolani, S., Bica, E., et al. 2003, A&A, 408, 127
Fang, K., & Halzen, F. 2024, JHEAp, 43, 140
Gabici, S., Evoli, C., Gaggero, D., et al. 2019, IJMPD, 28, 1930022
H.E.S.S. Collaboration, Abramowski, A., Aharonian, F., et al. 2016, Natur, 531, 476
Longair, M. S. 2010, High Energy Astrophysics (Cambridge: Cambridge Univ. Press)
Scherer, A., Cuadra, J., & Bauer, F. E. 2023, A&A, 679, A114
Strong, A. W., Moskalenko, I. V., & Ptuskin, V. S. 2007, ARNPS, 57, 285
Sudoh, T., & Beacom, J. F. 2023, PhRvD, 107, 043002
The CTA Consortium, et al. 2019, EPJ Web of Conferences
Tsuboi, M., Handa, T., & Ukita, N. 1999, ApJS, 120, 1
Vianello, G., Lauer, R., Younk, P., et al. 2016, in 34th Int. Cosmic Ray Conf. (ICRC2015) (Trieste: SISSA), 1042
Wilks, S. S. 1938, Ann. Math. Statist., 9, 60
Younk, P. W., Lauer, R. J., Vianello, G., et al. 2015, in 34th Int. Cosmic Ray Conf. (ICRC2015) (Trieste: SISSA),
Yusef-Zadeh, F., Hewitt, J. W., & Cotton, W. 2004, ApJS, 155, 421
Yusef-Zadeh, F., & Morris, M. 1987, ApJ, 322, 721